

## Phase transitions in driven lattice gases

J. Marro, A. Achahbar, P. L. Garrido, and J. J. Alonso\*

*Instituto Carlos I de Física Teórica y Computacional and Departamentos de Física Aplicada y Moderna, Facultad de Ciencias, Universidad de Granada, E-18071 Granada, Spain*

(Received 2 October 1995; revised manuscript received 1 March 1996)

We have studied nonequilibrium lattice gases whose particles are driven by a field. The lattice is either a half-occupied square lattice or else the union of two energetically uncoupled ones. Monte Carlo simulations of the latter, which is always crossed by a dissipative particle current, show a tricritical point and a continuum of Ising-like critical points as the field is decreased, in addition to non-Ising, anisotropic critical behavior at higher temperatures for saturating fields. A comparison of the various phase transitions involved, and a detailed study of scaling of correlations with system size, indicate the relevance of the anisotropic liquid-vapor interface (rather than the driving field) for inducing non-Ising behavior in a class of systems. It is likely that some of the properties reported here are experimentally observable. [S1063-651X(96)07506-X]

PACS number(s): 66.10.-x, 05.70.Fh, 64.60.Cn

### I. INTRODUCTION AND SOME DEFINITIONS

Stochastic lattice gases are suited to studying ordering phenomena in open systems such as pattern formation, self-organization, morphogenesis, etc. [1–3]. In particular, the *driven lattice gas* (DLG) is believed to capture some of the essential physics in a class of steady states with anisotropies. The DLG is a lattice gas with nearest neighbor (NN) attractions which evolves in time by stochastic NN particle-hole exchanges as induced by a heat bath at temperature  $T$ . Unlike the ordinary lattice gas, the DLG involves a driving external field,  $E\hat{x}$ , which causes preferential jumping of particles along one of the principal lattice directions,  $\hat{x}$ . Consequently, the resulting steady states are characterized, for periodic boundary conditions, by a net current of particles along  $\hat{x}$  for any  $E > 0$ ; this corresponds to a nonequilibrium, dissipative condition [4].

For the sake of simplicity, we only consider below the case in which  $E$  is constant and the bath is implemented by the Metropolis rule. The latter implies that the probability per unit time for the exchange of a particle and a hole depends on the corresponding energy cost. *Energy* is defined for this non-Hamiltonian system as the sum of the Ising Hamiltonian plus the work done by the field (only) for exchanges along  $\hat{x}$ . Consequently, the probability (per unit time) for a NN jump is  $p = \min\{1, \exp[-(\Delta H + E)/k_B T]\}$ , where  $\Delta H$  represents the variation of the Ising Hamiltonian due to the exchange and one sets  $E = 0$  (which reduces  $p$  to the familiar Metropolis rule) unless the particle-hole bond points  $+\hat{x}$  ( $-\hat{x}$ ), in which case  $E > 0$  ( $E < 0$ ). The lattice is a rectangle of  $N = L_x \times L_y$  sites with toroidal boundary conditions. Another simplifying restriction is that we only deal here with half-occupied lattices, i.e., the particle density is  $\rho = \frac{1}{2}$ .

This system is hereafter denoted  $\lambda_E$ ; it has been described

in more detail in Refs. [3,5], for instance. In addition to  $\lambda_E$ , we have studied  $\Lambda_E$ , which is the union of a pair of copies of  $\lambda_E$ ,  $\lambda_E^{(1)}$ , and  $\lambda_E^{(2)}$ , with corresponding sites,  $\mathbf{r}^{(1)}$  and  $\mathbf{r}^{(2)}$ , in the two copies connected insofar as particle jumping is concerned, but not energetically. In other words, a particle at  $\mathbf{r}^{(i)}$ ,  $i = 1, 2$ , may jump to one of five sites, one of which lies in the other copy. Jumping along either  $\hat{x}$  or  $\hat{y}$  in  $\Lambda_E$  follows the same rules as for  $\lambda_E$ , and jumping along  $\hat{z}$  (i.e., to the other copy) follows the Metropolis rule, as for  $\hat{y}$  jumps [3,6]. The cases of  $\lambda_E$  and  $\Lambda_E$  for which the field is *saturating*, which means that no particle may perform  $-\hat{x}$  jumps, are denoted  $\lambda_\infty$  and  $\Lambda_\infty$ , respectively.

Previous Monte Carlo (MC) studies have revealed the main features of ordering in these models, and how they sometimes reproduce the behavior in nature. For example, the net particle current which occurs in the models for any  $T > 0$  reminds one of the current of ions in *fast ionic conductors* [7]. In the case of  $\lambda_\infty$  and  $\Lambda_\infty$ , the current exhibits a sudden break of slope which marks a critical point located at temperature  $T_\infty$ . The latter equals approximately  $1.4T_0$  and  $1.3T_0$  ( $T_0$  is the—equilibrium—Ising critical temperature for dimension  $d = 2$ ) for  $\lambda_\infty$  and  $\Lambda_\infty$ , respectively. It is very likely that similar folds and other anomalies observed before in the conductivity-versus- $T$  curve of many substances have the same origin, i.e., they mark the onset of a (nonequilibrium) phase transition [3]. For  $T < T_\infty$ , the models exhibit a liquid, particle-rich phase which coexists with its vapor. A novel feature is that this liquid happens to be striped, and the interface is linear parallel to  $\hat{x}$ . It seems natural to argue that similar anisotropic interfaces, and perhaps some of the specific properties of  $\Lambda_E$ , might be exhibited by certain materials in which the currents occur within restricted, e.g., two or quasi-two-dimensional geometries. This endows the study of  $\lambda_E$  and  $\Lambda_E$  with some practical interest. Comparing with each other the behavior of these systems (which was initiated in Refs. [6,8]) is also interesting because of the extremely slow evolution typical of most lattice gases. That is, very slow relaxation hampers in practice the MC simulation of  $\lambda_E$  for any  $E \geq 0$  while the evolution may be accelerated in  $\Lambda_E$  where density fluctuations have an additional mode of

\*Present address: Laboratoire de Physique et Mécanique des Milieux Hétérogènes, Ecole Supérieure de Physique et Chimie Industrielles, 10 rue Vauquelin, 75231 Paris Cedex 05, France.

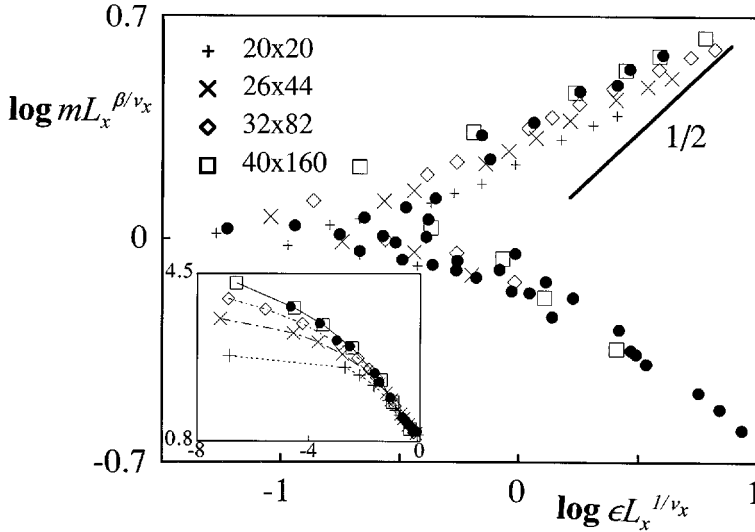


FIG. 1. MC data corresponding to the order parameter  $m$  for different sizes, as indicated, are compared with field-theoretic predictions, Eq. (2). Here  $\beta = \frac{1}{2}$ ,  $\nu_x = \frac{3}{2}$  and further details as suggested in Ref. [14] (from where the data for the black dots—which correspond to different sizes—have been taken), and  $T_\infty = 1.38$  as obtained independently from both cumulants and specific heat. No scaling behavior is observed, nor does the slope  $\frac{1}{2}$  seem to be of any significance (cf. Ref. [6] for further evidence). The same occurs for  $T_\infty = 1.418$  (used in Ref. [14]) as illustrated by the inset (where decimal logarithms are avoided) below  $T_\infty$ . (Temperatures are always in units of the 2D Ising critical temperature,  $T_0$ , except for mean-field results as reported in Figs. 4 and 5, and  $\rho = \frac{1}{2}$ ; logarithms are decimal.)

relaxation, namely, jumping of particles to the other lattice [9].

There is also a more fundamental interest for  $\lambda_\infty$  and  $\Lambda_\infty$ . In particular, one would like to investigate the universality class for the phase transitions in these systems, and its relationship with the universality class for the equilibrium counterparts,  $\lambda_0$  and  $\Lambda_0$ , i.e., the influence the underlying anisotropy has on critical behavior. This issue has been addressed by field theory based on the proposal that a Langevin-like equation with a drift is the continuous version of  $\lambda_\infty$  [10–12]. Assuming that the field operator is *relevant*, renormalization group (RG) techniques near  $T_\infty$  produce a solvable—classical—case for  $2 < d \leq 5$ . This provides an interesting description of anisotropy and critical behavior. In particular, the existence of two independent correlation lengths diverging with distinct exponents, e.g.,  $\nu_x = \frac{3}{2}$  and  $\nu_y = \frac{1}{2}$  for  $d=2$ , is predicted. It has led before to the expectation that the DLG should behave isotropically if the ratio  $L_x^{\nu_x/\nu_y} L_y^{-1}$  is fixed. More explicitly, consider the *ensemble average* of the *local density* [13,14], defined as the MC stationary average (denoted  $\langle \dots \rangle$ ) of

$$\phi \equiv \frac{1}{2L_x} \sin\left(\frac{\pi}{L_y}\right) \left| \sum_{x=0}^{L_x-1} \sum_{y=0}^{L_y-1} (1 - 2\sigma_{x,y}) e^{ik \cdot \mathbf{r}} \right|, \quad (1)$$

where  $\sigma_{\mathbf{r}} = 0, 1$  and  $\mathbf{k} = (0, 2\pi L_y^{-1})$ ; a specific prediction is that  $m \equiv \langle \phi \rangle$  behaves as

$$m = L_x^{-\beta/\nu_x} \tilde{m}(\varepsilon L_x^{1/\nu_x}), \quad (2)$$

where  $\varepsilon \equiv (T - T_\infty) T_\infty^{-1}$ .

There is a claim that these expectations are supported by MC data [14,15]. Systematic departures from (2) have been reported [6,16–18], however, and data obstinately fit the behavior  $m \sim \varepsilon^{-\beta}$  with  $\beta \approx 0.3$  near  $T_\infty$  for large enough systems. On the contrary, the field-theoretic prediction that  $\beta = \frac{1}{2}$ , *perhaps with weak logarithmic corrections* for the (*marginal*) case  $d=2$ , is not confirmed in general. Figure 1 illustrates how data depart from the prediction (2). The existence of critical points which are characterized by an order-parameter critical exponent  $\beta$  whose value is apparently between the classical ( $\frac{1}{2}$ ) and equilibrium ( $\frac{1}{8}$ ) values has also

been reported for a number of different but very closely related systems. For example, we are aware this has been observed for a different case of lattice gas with anisotropic dissipative flow [19], for some modifications of  $\lambda_\infty$ , which include either anisotropic couplings [20] or else spin flips at a smaller rate than the exchanges in order to accelerate relaxation [17], for the case of a lattice gas under shear [21], for the lattice gas in which  $+\hat{x}$  and  $-\hat{x}$  jumps occur completely at random with same probability [22,23], and for the two-layer system  $\Lambda_\infty$  [6].

Therefore some questions concerning the nature of the underlying anisotropy and its influence on emergent properties arise. It is important to compare the just mentioned systems with each other, and to determine what are the essential ingredients for DLG behavior (and whether they are contained in the continuous model or not). More generally, one would like to consider the issue of universality for these nonequilibrium systems. We have addressed such problems by comparing  $\lambda_E$  and  $\Lambda_E$  (which has been shown to be interesting even for  $E=0$  [9]) by means of MC analysis and mean-field (and other) arguments. It has clarified the nature of various phase transitions. In particular, we describe below two different critical points in  $\Lambda_E$ . One of them occurs for a saturating field at  $T_\infty (> T_0)$ ; this is of the same (rare) class as the one in  $\lambda_\infty$ . The other critical point occurs in  $\Lambda_E$  (but not in  $\lambda_E$ ) for finite  $E$  at a field-dependent temperature below  $T_0$ ; this is of the Ising variety, as for  $\lambda_0$ . The segregation in this case is such that no liquid-vapor interface exists. Therefore, the (anisotropic) interface which develops just below  $T_\infty$  may be at the origin of the peculiar, non-Ising critical and scaling behavior of the DLG above  $T_0$ . We believe that the non-Ising critical properties of the models should be experimentally observable in nature. In order to clarify the relevant role played by the interface, we have studied further the scaling of correlations in the DLG. A question one should try to clarify here is whether there is a single scaling length or else two lengths associated, respectively, with each of the two principal lattice directions. We present a simple description of the variations of the order parameter with system size, which just involves the existence of a unique scaling length. On the other hand, assuming that two lengths are needed to describe clusters and other inhomogeneities which

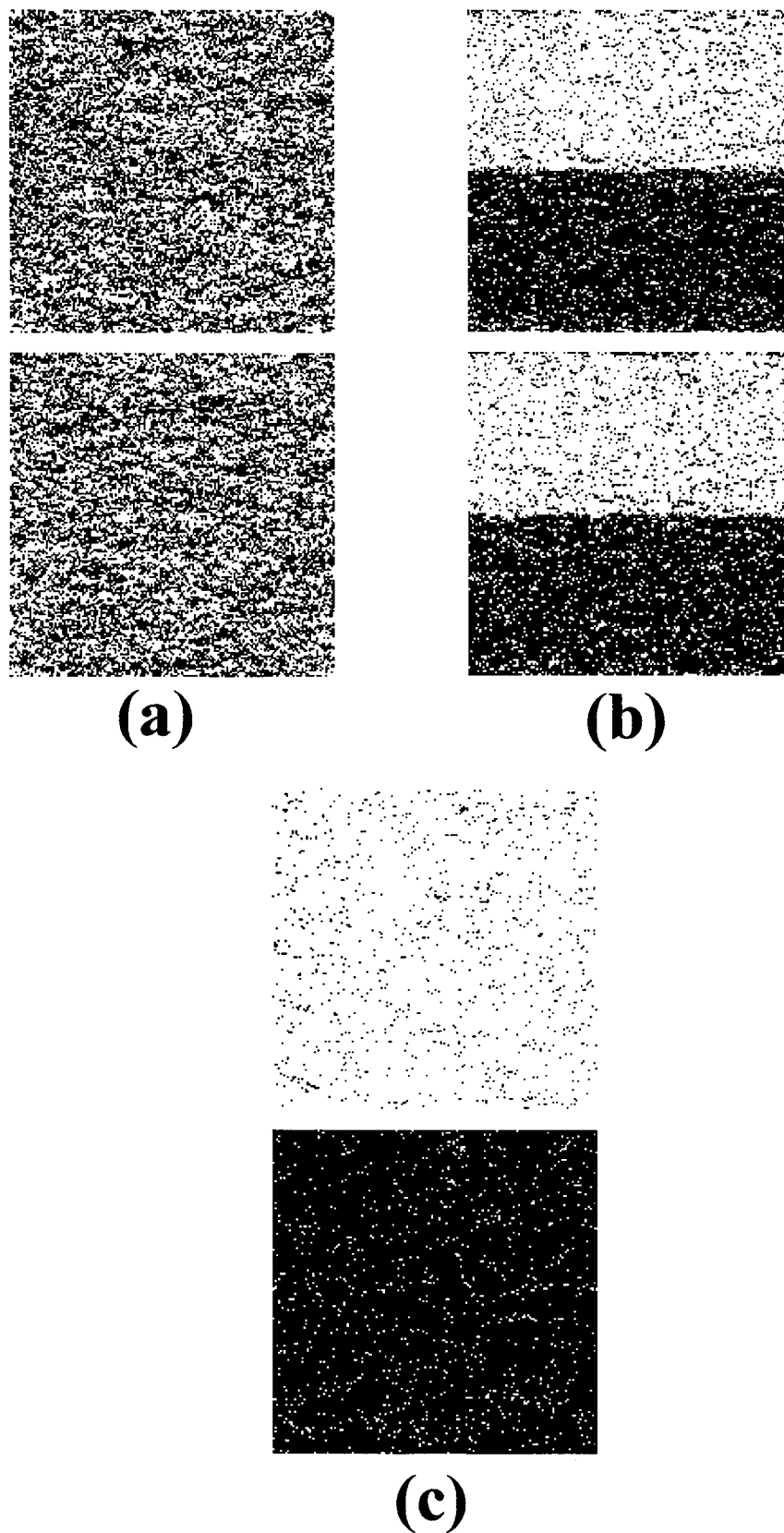


FIG. 2. Some typical configurations obtained for the two planes of  $\Lambda_\infty$  by the MC method for the  $2 \times 200 \times 200$  lattice, a saturating field acting horizontally, and (a)  $T = 1.5 > T_\infty$ , (b)  $T = 1.1$ , i.e.,  $T_\infty > T > T_\infty^*$ , and (c)  $T = 0.85 < T_\infty$ . Small anisotropic clusters may be detected by direct inspection. The phase transition which separates (a) from (b) is continuous with peculiar critical behavior; the one which separates (b) from (c) is discontinuous but it becomes continuous with Ising-like critical behavior for small enough values of the field.

are observed to occur in the systems, MC data indicate that they are not independent of each other. None of these observations appear to be consistent with the field-theoretic assumption that the field is relevant in the sense of RG theory.

## II. ORDERING AND CRITICAL POINTS

For reference, Fig. 2 illustrates three types of ordered states which occur in  $\Lambda_\infty$ , and the two distinct (nonequilibrium) phase transitions that are involved. A few facts are to be emphasized. For temperatures above  $T_\infty$  (particle density is fixed at  $\rho = \frac{1}{2}$  throughout this paper), steady states are homogeneous on a large spatial scale but show clear anisotropies on smaller scales. More specifically, clusters that are stretched out along  $\hat{x}$  are often observed even by direct inspection, as in Fig. 2(a). As described above,  $T_\infty$  seems to correspond (for the macroscopic system) to a critical point below which the layered system segregates into coexisting liquid and gas phases. Figure 2(b) illustrates that the two planes of  $\Lambda_\infty$  exhibit the same type of order, i.e., coexisting states, for any  $T$  within the range  $T_\infty > T > T_\infty^*$ . Nevertheless, such symmetry between planes breaks down below  $T_\infty^*$ , which marks the onset of phase transitions that are first-order-like, i.e., discontinuous for a saturating field (see below, however). Each plane is filled below  $T_\infty^*$  by one of the phases, either liquid or gas only; cf. Fig. 2(c). The pure phases for  $T < T_\infty$  (i.e., including the ones for  $T < T_\infty^*$ ) exhibit well-defined anisotropies, as for  $T > T_\infty$ . One may become convinced of this fact by careful direct inspection of graphs such as the ones in Fig. 2, and it has been proved numerically after studying the relevant correlation functions (cf. figure 10 of Ref. [6]). Consistently with this, it has been argued that one effect of the field is transforming equilibrium ( $E=0$ ) liquid clusters roughly from spherical to triangular (for appropriate values of  $\rho$  and  $E$ ) [24]. Summing up, two main questions ensue from MC simulations that deserve further study: (i) the apparent existence of two lengths, and the influence of this fact on critical behavior, and (ii) the relation between the phase transitions exhibited by  $\lambda_E$  and  $\Lambda_E$ . We address the latter problem first; (i) is discussed in detail in Sec. III.

To perform quantitative comparisons, one may monitor order parameter and *energy*, for instance. A natural way of measuring anisotropic ordering for  $\rho = \frac{1}{2}$  is to compute the average of (1),  $m$ . The (anisotropic) *squared magnetization* [4]

$$M \equiv \sqrt{|(M_x^2) - (M_y^2)|}, \quad (3)$$

where

$$M_{x(y)}^2 \equiv \frac{1}{L_x \times L_y \times L_{x(y)}} \sum_{y(x)=1}^{L_{y(x)}-1} \left[ \sum_{x(y)=1}^{L_{x(y)}-1} (1 - 2\sigma_{x,y}) \right]^2, \quad (4)$$

has also been studied. Both  $M$  and  $m$  are normalized such that they equal unity for the zero-temperature configurations. For  $\rho = \frac{1}{2}$  (the only case which is of interest here),  $M$  and  $m$  have been defined for  $\Lambda_E$  as an average of the corresponding quantity over the two planes. Furthermore, measuring the density of each phase,  $\rho_{gas}(T)$  and  $\rho_{liquid}(T)$ , and the difference of density between the two planes of  $\Lambda_E$ ,

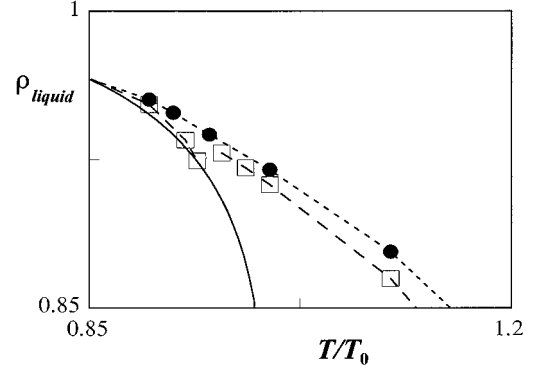


FIG. 3. The particle density of the pure phase,  $\rho_{liquid}(T)$ , as obtained for  $\lambda_\infty$  (●) and  $\Lambda_\infty$  (□) using lattices of comparable size, and the corresponding Onsager exact result (solid line); dashed lines are a guide to the eye. (The neighborhood of the respective critical regions, where it becomes difficult to accurately define in practice the phases in MC simulations, is not shown.)

$$\Delta\rho = \frac{1}{2\rho} |\langle \rho_1(T, \rho) \rangle - \langle \rho_2(T, \rho) \rangle|, \quad (5)$$

is interesting. In the following,  $\psi$  stands for any of these quantities, namely,  $\psi = m, M, \Delta\rho$ , etc. In fact, even though each of them corresponds to a different measure of correlations, their stationary values should not differ from each other sufficiently near the critical point (the region of most interest here), which is indeed confirmed below.

We first mention that one should expect the critical point at  $T_\infty$  in  $\Lambda_\infty$  to be identical to the more familiar one in  $\lambda_\infty$ . This is already suggested by the fact that there is a strong similarity of segregated states; e.g., close direct inspection does not reveal any systematic qualitative differences between the planes in Fig. 2(b) and corresponding configurations of  $\lambda_\infty$ . Furthermore, both systems have been demonstrated to have the same critical point for  $E=0$  [9], and the symmetries which are introduced for any  $E>0$  by dynamics in  $\Lambda_E$  are already present in  $\lambda_E$ . That is,  $\lambda_E$  and  $\Lambda_E$  are characterized by the same (microscopic) dynamical rule, and it has been observed to produce the same type of (macroscopic) interface in both systems. Therefore, we are assuming in the following that  $\Lambda_\infty$  and  $\lambda_\infty$  have the same critical point, which seems confirmed by all the available MC data, as discussed below.

However, some important differences between  $\lambda_E$  and  $\Lambda_E$  should be expected. This is illustrated by the behavior of  $\rho_{liquid}(T)$  in Fig. 3. In addition to the fact that the liquid density is, in general, larger in the presence of the field, which is due to different behavior of correlations [6], one observes in Fig. 3 that  $\rho_{liquid}(T)$  is definitely larger for  $\lambda_\infty$  than for  $\Lambda_\infty$ . One might argue this is simply related to the fact that the systems are finite, and  $\rho$  is the same in both cases for given  $T$ . Nevertheless, kinetic mean-field (numerical) methods which have been developed before [5,8] demonstrate a more essential difference between  $\lambda_E$  and  $\Lambda_E$ . A first argument is as follows. Consider, as a measure of energy, the density of particle-hole pairs,  $e_{\Lambda_E}$ , within the disordered phase of  $\Lambda_E$  at high enough temperature. The time variation of  $e_{\Lambda_E}$  may be written quite generally within the

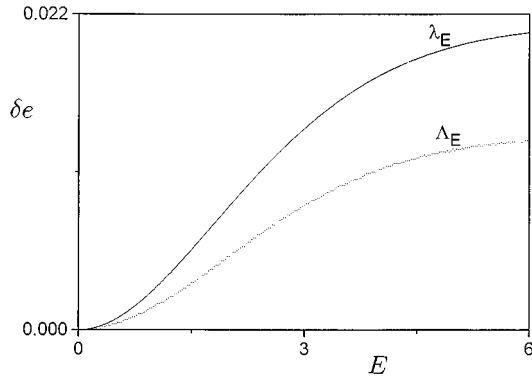


FIG. 4. Field dependence for a typical value of the temperature [namely,  $T=3.2(J/k_B)$ ] of  $\delta e \equiv e_x - e_y$ , the difference between the density of particle-hole pairs along  $\hat{x}$  and that along  $\hat{y}$ , for systems  $\lambda_E$  and  $\Lambda_E$  as indicated. This has been obtained numerically from the kinetic mean-field theory in Ref. [8]. (The field is dimensionless throughout this work; see the main text in Sec. I for details.)

pair approximation as the sum of two terms,  $I_1$  and  $I_2$ , which describe the particle-hole exchanges within each plane, and a third term,  $I_{1=2}$ , which describes interplane exchanges (some further details that are not needed here may be found in Ref. [8]). The stationary solution for one plane,  $e_{\lambda_E}$ , cancels out both  $I_1$  and  $I_2$  for any  $E \geq 0$  while it turns out that this causes  $I_{1=2}$  to vanish only for  $E=0$  because of some field dependence within the dynamical rate. Therefore, one has  $\partial e_{\Lambda_E}(t)/\partial t = 0$  for  $t \rightarrow \infty$  due to cancellations between  $I_1$ ,  $I_2$ , and  $I_{1=2}$  and, as a consequence,  $e_{\Lambda_E}$  and  $e_{\lambda_E}$  differ in general from each other for any  $E > 0$ , i.e., the corresponding steady states are not identical.

Mean-field theory also indicates that the difference of  $e$  between the  $\hat{x}$  and  $\hat{y}$  directions is generally smaller for  $\Lambda_E$  than for  $\lambda_E$ ; this is shown in Fig. 4. That is, the existence of the other plane causes anisotropy to decrease. It may be understood if one thinks of dynamics for  $\lambda_E$  as consisting of a competition between the field, on the one hand, and a thermal process along  $\hat{y}$ , on the other. Then extra thermal randomness (along  $\hat{z}$ ) adds to this for  $\Lambda_E$  that (slightly) compensates the anisotropic action of the field. If this argument is right, one should expect  $T_E^\lambda > T_E^\Lambda$ , which is indeed a direct result from mean-field computations, as illustrated by the upper curves in Fig. 5. The same is supported by MC simulations for saturating fields, which definitely indicates that  $T_\infty^\lambda - T_\infty^\Lambda > 0$  beyond statistical errors. This is demonstrated in Fig. 6, which describes the size and temperature dependence of the cumulant [17]:

$$g_L = \frac{4}{3} \left[ 1 - \frac{\langle \phi^4 \rangle}{2 \langle \phi^2 \rangle^2} \right]. \quad (6)$$

(Further support follows from the behavior of  $\rho_{liquid}$  in Fig. 3.) It also ensues from this interpretation of dynamics in terms of a competition between two effects that, as concluded above, the same critical behavior should be expected (as for  $E=0$ ) for both  $\lambda_\infty$  and  $\Lambda_\infty$ ; that is, no new effects nor symmetries are introduced by such a dynamical process in  $\Lambda_\infty$  as compared to the case of  $\lambda_\infty$ . As a matter of fact, the only hypothesis that seems to describe correctly the *critical*

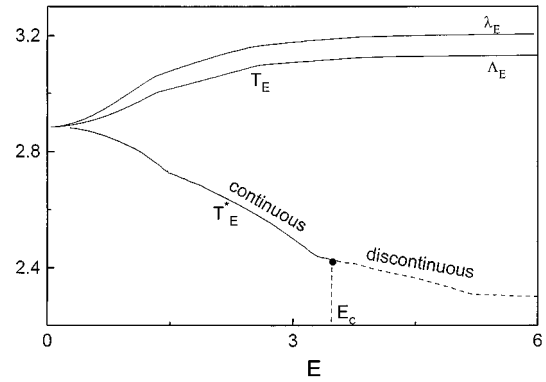


FIG. 5. Field dependence of transition temperatures [in units of  $(J/k_B)$ ]; the graph, which is adapted from Ref. [8], illustrates up to the case of a saturating field. The upper curves are for  $\lambda_E$  and  $\Lambda_E$ , as indicated; the latter corresponds to the phase transition at  $T_E$  between states such as the one in Fig. 2(a) and the one in Fig. 2(b). The lower curve corresponds to the coagulation of the liquid in only one of the planes of  $\Lambda_E$ , i.e., the transition at  $T_E^*$  between states such as the one in Fig. 2(b) and the one in Fig. 2(c). The (nonequilibrium) tricritical point which characterizes  $\Lambda_E$  is indicated.

region, namely, the closest neighborhood of the critical point that has been accessible so far by the MC method, is  $\psi \sim \varepsilon^{-\beta}$  with  $\beta \approx 0.3$  for both  $\lambda_\infty$  and  $\Lambda_\infty$ ; this is demonstrated in Fig. 7 (see also Refs. [6,16]). Figure 7 suggests that the two systems have the same critical thermodynamic amplitude as well.

As a confirmation of the above, we have obtained some evidence from a few MC short runs that the *a priori* interplane rate influences somewhat the transition temperature of  $\Lambda_\infty$ . (In fact, we have observed that currents are a fundamental ingredient in this system. We believe, in particular, that interplane currents are responsible for the phase transition at  $T_\infty^* \approx 0.95 < T_\infty$ , which is indicated in Figs. 2 and 3.) The same picture ensues from mean-field theory, which demon-

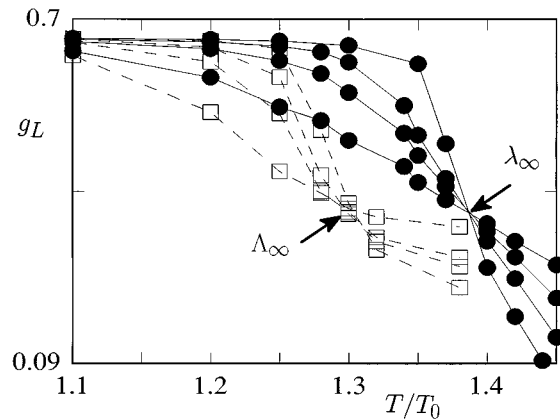


FIG. 6. The dependence with size and temperature of the (dimensionless) cumulant (6) for  $\lambda_\infty$  (●) and  $\Lambda_\infty$  (□); the crossings here locate the corresponding critical temperature [17], as indicated. The four different sizes presented here are  $20 \times 20$ ,  $26 \times 44$ ,  $32 \times 82$ , and  $40 \times 160$ , respectively, for both  $\lambda_\infty$  and  $\Lambda_\infty$ . This plot suggests  $T_\infty^\lambda \approx 1.38$  and  $T_\infty^\Lambda \approx 1.30$  in accordance with other evidence. Lines are a guide to the eye.

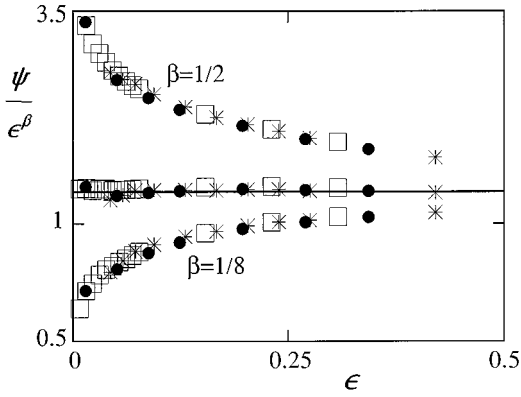


FIG. 7. Temperature dependence of  $\psi\epsilon^{-\beta}$  for different assumptions about  $\beta$ , as indicated. Data for  $\psi$  correspond to the magnetization  $M$  for  $\lambda_\infty$  (asterisks) and  $\Lambda_\infty$  ( $\square$ ) (both are extrapolations to infinite size obtained from squared lattices by the method in Ref. [16]), and to the local density  $m$  for  $\lambda_\infty$  ( $\bullet$ ) (for the  $40 \times 160$  lattice). The only three sets of symbols which exhibit independence of temperature near  $\epsilon = 0$  (which turn out to be fitted by the solid line corresponding to  $B = 1.24$ ) are for  $\beta = 0.27$ , and  $T_\infty^\lambda = 1.38$  (asterisks),  $T_\infty^\Lambda = 1.30$  ( $\square$ ), and  $T_\infty^\lambda(L) = 1.37$  ( $\bullet$ ).

states that the transition at  $T_\infty^*$  not occurring in  $\lambda_\infty$  depends crucially on the dynamical rule. More explicitly, it has been reported [8] that the Metropolis rule, but not other familiar choices, induces the existence of a nonequilibrium tricritical point. This means that the phase transition at  $T_E^*$  is discontinuous for  $E$  large enough (as observed in MC simulations for saturating field), while it becomes continuous for small enough  $E$ . The point separating these two types of behavior is estimated by the mean-field approximation to be at  $E = E_c = 3.5 \pm 0.1$ ; cf. Fig. 5.

The latter result has moved us to perform a systematic MC study of  $\Lambda_E$  for varying values of  $E$  and  $T$ . The data confirm the above. In particular, the existence of a critical point (for  $\rho = \frac{1}{2}$ ) at  $T_E^*$  for any  $E < E_c \approx 2$  has been demonstrated. Interestingly enough, these critical points seem to be

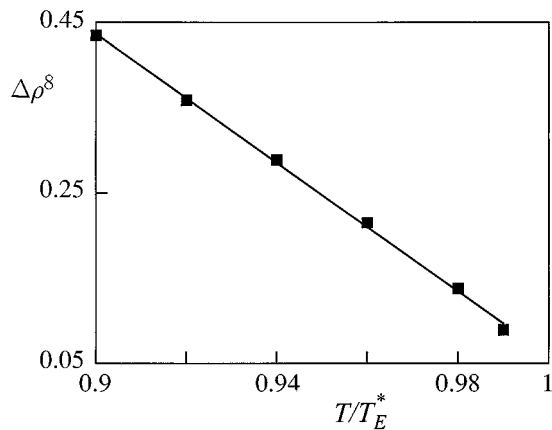


FIG. 8. A plot of the difference of particle density between the two planes of  $\Lambda_E$ , as defined in Eq. (5), near  $T_E^* (= 0.95T_0)$  to illustrate consistency with an order-parameter exponent  $\beta = \frac{1}{8}$  for  $E = 1$  (the field is dimensionless; cf. Fig. 4). The data were obtained from MC simulations of the  $128 \times 128$  lattice; the solid line corresponds to the predicted linear behavior.

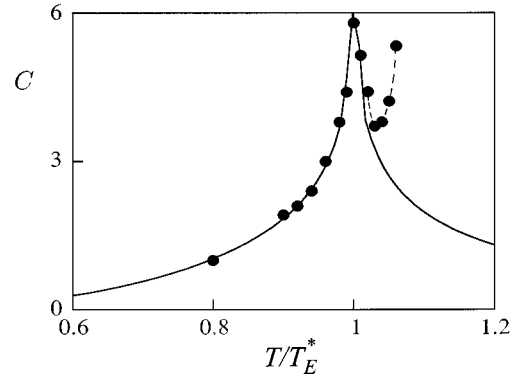


FIG. 9. A comparison of equilibrium and nonequilibrium specific heats: the solid line is the Onsager exact result and the dots correspond to mean squared fluctuations of the energy  $e$  (from the MC simulations reported in Fig. 8 for  $E = 1$ ). The high-temperature phase transition which occurs at  $T_E$  is suggested by data for  $T > T_E^*$ . The energy  $e$  is defined as the probability of a particle-hole pair in the system.

of the Ising class. Some indication of this is given in Fig. 8, which suggests  $\beta = \frac{1}{8}$ . Even more convincing is perhaps Fig. 9, which shows quite a consistency of data for energy fluctuations with the specific heat function corresponding to the Onsager solution. This simplicity of behavior at  $T_E^*$  for  $E < E_c$  was a surprise to us. That is, one is dealing here with a full nonequilibrium state in the sense (e.g.) that a (dissipative) particle current exists, as illustrated in Fig. 10, but the behavior is much simpler than near  $T_\infty$ . For instance, no such fit, which suggests that a fluctuation-dissipation relation holds, has ever been observed so far around  $T_\infty$ . Incidentally, we mention that Fig. 10 suggests a change of slope near the transition at  $T_E^*$  which is similar to the one often reported for fast ionic conductors.

### III. CORRELATIONS AND SCALING BEHAVIOR

We turn now to the scaling properties of correlations and, in particular, to the intriguing question about the apparent existence of two correlation lengths; cf. first paragraph of the

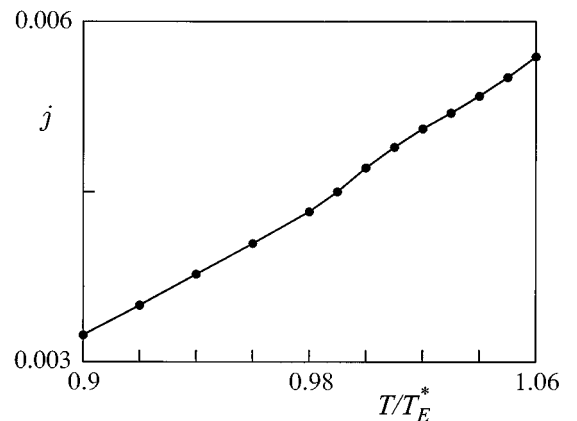


FIG. 10. Temperature dependence for  $E = 1$  (cf. Fig. 4 caption) of the particle current, namely, stationary average of the net number of particles crossing any  $\hat{y}$  section per unit time in direction  $+\hat{x}$  divided by  $N$ , as obtained from the MC simulations in Fig. 8.

preceding section. The consideration of these matters happens to clarify further the relation between  $\lambda_E$ ,  $\Lambda_E$ ,  $\lambda_0$ , and  $\Lambda_0$ . Let us denote by  $l_x$  and  $l_y$ , respectively, the two lengths which seem to be needed to characterize the anisotropies which are exhibited by the DLG for any value of  $T$  and  $E$ . In fact, anisotropic clusters have explicitly been reported before both at high  $T$  [6,8] for any  $E$  and at low  $T$  [24] for small  $E$ . It is our belief that  $l_x$  and  $l_y$  depend on each other. Our argument may be made explicit for large  $E$  at low  $T$ , for example. Then one may interpret the lengths, respectively, as the mean displacement along  $\hat{\mathbf{x}}$  and  $\hat{\mathbf{y}}$  of a hole (particle) within the striped liquid (gas) during a time interval  $\Delta t$ . If the two processes are independent of each other, one may imagine that a random walk occurs along the  $\hat{\mathbf{y}}$  direction, i.e.,  $l_y^2 \sim D\Delta t$ , where  $D$  is the diffusion coefficient. However, one should expect longitudinally that  $l_x \sim v\Delta t$  with  $v$  corresponding to the (terminal) velocity due to the applied field. Therefore, the expectation is that  $l_x \sim l_y^2$ . One may analyze quantitatively this possibility by assuming that correlations behave, approximately, as

$$G(x,y) \sim \frac{ax^2 - by^2}{(x^2 + y^2)^2} \quad (7)$$

for *sufficiently large* distances. On this assumption one obtains that  $a \sim b^\varsigma$  with  $\varsigma \approx 2$  over the whole range of temperatures investigated [16,6], in accordance with our expectation.

This observation may be interpreted as indicating that the shape of the (anisotropic) clusters is in practice determined for each given value of  $E$ , and the relation between the two lengths is then maintained as  $T$  is varied. Therefore, the existence of a unique relevant correlation length,  $\xi$ , near  $T_\infty$  is suggested whose relation with the other lengths may be imagined to be roughly

$$\xi \sim \sqrt{l_x l_y} \sim l_y^{\frac{\varsigma+1}{2}}, \quad \varsigma \approx 2, \quad (8)$$

for example. This explains that  $l_x$  may not contribute to the critical and scaling behavior of the DLG; only  $l_y$ , which is essentially mediated by the existence of the interface along  $\hat{\mathbf{x}}$ , matters. A similar situation has been reported for (self-affine) interface phenomena [25]. Self-affinity has been shown to imply in the critical point of some growth models a logarithmic behavior which has indeed been observed to characterize the size fluctuations of the interface of the DLG [26,15].

The above suggests that anisotropic critical behavior is not a consequence of two correlation lengths but of the properties of the interface. This fact may explain also the DLG scaling properties which have been reported before. To see this, let us assume (against our belief) that two relevant lengths exist, and consider the Hamiltonian

$$H = \int d\mathbf{r} [(\nabla \psi)^2 + \varepsilon \psi^2 + u \psi^4], \quad u > 0, \quad (9)$$

for instance. Following standard reasoning and notation [27,28], the pair correlation function is

$$G(x,y;\varepsilon,u) = \lambda^{\Delta+\eta} G(\lambda^{1+\Delta} x, \lambda y; \varepsilon \lambda^{-1/\nu}, u \lambda^{\theta/\nu}). \quad (10)$$

Then using  $\lambda = \varepsilon^\nu$  here gives the correlation lengths as  $\xi_x \sim \varepsilon^{-\nu(1+\Delta)}$  and  $\xi_y \sim \varepsilon^{-\nu}$  for  $\varepsilon \rightarrow 0$ , and  $(\Delta + \eta)\nu = 2\beta$ . It ensues therefore that one should have rather generally below  $T_\infty$  that

$$\psi(L_x, L_y; \varepsilon, u) = \varepsilon^\beta \psi(L_x^{-1} \varepsilon^{-\nu(1+\Delta)}, L_y^{-1} \varepsilon^{-\nu}; 1, u \varepsilon^\theta). \quad (11)$$

Let us assume also that one may write

$$\psi(L_x, L_y; \varepsilon, u) \approx \psi(\varepsilon, u) + L_x^{-1} X(\varepsilon, u) + L_y^{-1} Y(\varepsilon, u) \quad (12)$$

to first order for large enough size. One has after combining this with (11) that

$$X(\varepsilon, u) = \varepsilon^{\beta-\nu(1+\Delta)} X(1, u \varepsilon^\theta), \quad (13)$$

$$Y(\varepsilon, u) = \varepsilon^{\beta-\nu} Y(1, u \varepsilon^\theta). \quad (14)$$

Assuming  $\Delta \approx 0$ , as implied by our arguments above, one therefore has below  $T_\infty$  that

$$\psi(L_x, L_y; \varepsilon, u) \approx B \varepsilon^\beta + \varepsilon^{\beta-\nu} \left[ \frac{X(1, u \varepsilon^\theta)}{L_x} + \frac{Y(1, u \varepsilon^\theta)}{L_y} \right], \quad T < T_\infty. \quad (15)$$

The first confirmation of this kind of finite-size correction in nonequilibrium anisotropic systems is probably in Ref. [16]. It was remarked there that the dependence of the order parameter  $M$  on the side  $L$  of  $\lambda_\infty$  conforms to  $M \sim L^{-1}$  for  $T < T_\infty$ , and  $M \sim L^{-\omega}$  with roughly  $\omega \approx 0.2$  for  $T > T_\infty$ . Consequently, the proposal for squares was that

$$\psi \sim \begin{cases} L^{-\beta/\nu} (B \kappa^\beta - B_s \kappa^{\beta-\nu}) & \text{for } T < T_\infty \\ B'_s \kappa^{-\omega\nu} & \text{for } T > T_\infty, \end{cases} \quad (16)$$

where  $\kappa \equiv \varepsilon L^{1/\nu}$ . The fact that this is an excellent description of data for both  $\lambda_\infty$  and  $\Lambda_\infty$  is illustrated in Fig. 11. Interesting enough, the empirical observation in (16) for  $T < T_\infty$  corresponds to (15) with

$$-B_s = X(1, u \varepsilon^\theta) + Y(1, u \varepsilon^\theta) \quad (17)$$

only if  $\Delta$  is zero or sufficiently small (and  $L_x = L_y$ ). One cannot conclude so generally above  $T_\infty$  because the parameter  $\omega$  in (16) turns out to be model dependent; cf. caption for Fig. 11.

Checking (15) for rectangles ( $L_x \neq L_y$ ) would require high quality data for many different shapes; we only consider here squared geometries, which is much more convenient. In any case, squares have provided us an even more stringent test of the validity of (15) than the one in Fig. 11. This is illustrated in Fig. 12, in which the finite-size corrections are isolated from the bulk (unlike in Fig. 11). One obtains from the analysis in Fig. 12 for the quantity  $M$  corresponding to  $\Lambda_\infty$  that  $B \approx 1.24$ , and that  $X(1, u \varepsilon^\theta) + Y(1, u \varepsilon^\theta)$  is constant, implying  $B_s \approx 1.1$ , for  $1 < \xi \sim \varepsilon^{-\nu} < L$ ; these values for  $B$  and  $B_s$  agree well with previous estimates in Ref. [16]. Figure 12 also reveals the expected departure from scaling for the *unphysical* region  $\xi > L$ . Interesting enough, the corrections in (15) turn out to have different sign, namely,  $X(1, u \varepsilon^\theta) > 0$ ,  $Y(1, u \varepsilon^\theta) < 0$ ; cf. below. The above formulas

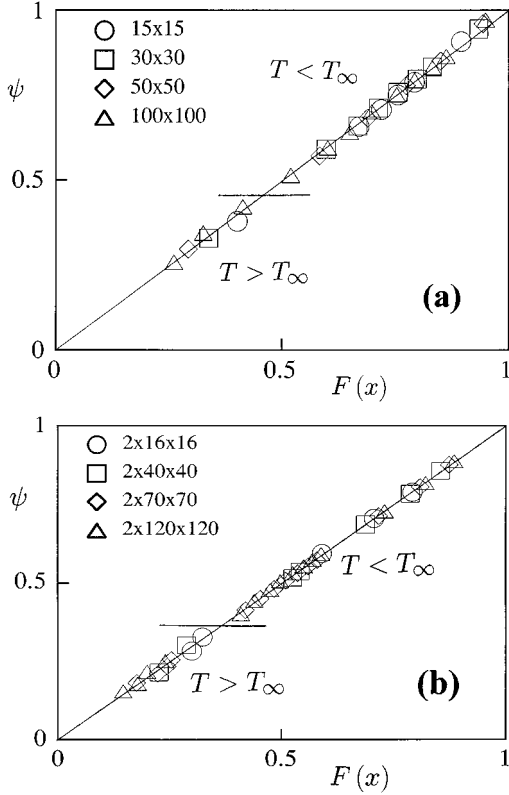


FIG. 11. The (dimensionless) order parameter *versus* the right-hand side of Eq. (16) for different sizes and systems, as indicated. The values for the parameters, to which the plot turns out to be very sensitive, have been obtained by the method in Ref. [16]. These graphs refer to  $\beta=0.27$  and  $\nu=0.7$ , and (a)  $T_\infty=1.38$ ,  $\omega=0.2$ ,  $B=1.24$ ,  $B_s=0.8$ , and  $B'_s=0.33$  for the case of  $\lambda_\infty$  that includes all available data for  $7 < \kappa < 200$  below  $T_\infty$  and  $\kappa > 7$  above  $T_\infty$ , and (b)  $T_\infty=1.3$ ,  $\omega=0.3$ ,  $B=1.24$ ,  $B_s=1.1$ , and  $B'_s=0.38$  for the case of  $\Lambda_\infty$  including all data for  $10 < \kappa < 300$  below  $T_\infty$  and  $\kappa > 3$  above  $T_\infty$ . The data outside the indicated ranges which deviate from (16), as expected (see the explanation below), are not included here.

cannot be fitted to data if the values  $\beta=\frac{1}{2}$  and  $\nu=\frac{3}{2}$  that characterize the continuous model [15] are used instead of the values reported here.

In order to see further consequences of (11)–(14), we remark that it is implied for  $\Delta \neq 0$  that

$$\frac{X(\varepsilon, u)}{Y(\varepsilon, u)} = \varepsilon^{-\Delta\nu} f(1, u \varepsilon^\theta). \quad (18)$$

This provides an explicit method for estimating the value of  $\Delta$ , and one may check the field-theoretic prediction,  $\Delta=2$  or  $\Delta\nu=1$ . We have estimated  $X/Y$  from the behavior of  $m$  for the layered system. That is, several sets of data, each corresponding to a different lattice size and shape, have been combined with (12) to obtain  $X/Y$  by the least squares method. The main result is illustrated in Fig. 13. This, confirming the other evidence, may be interpreted as an indication that no singularity occurs in (18) as  $\varepsilon \rightarrow 0^-$ . It rather suggests that  $\Delta=0$  given that the bound  $|X/Y| < 1$  is indicated, and one obtains from the physical region  $1 < \xi < L$  in this figure that  $X/Y \approx 0.28\varepsilon - 0.98$  near the critical point for the finite-size corrections.

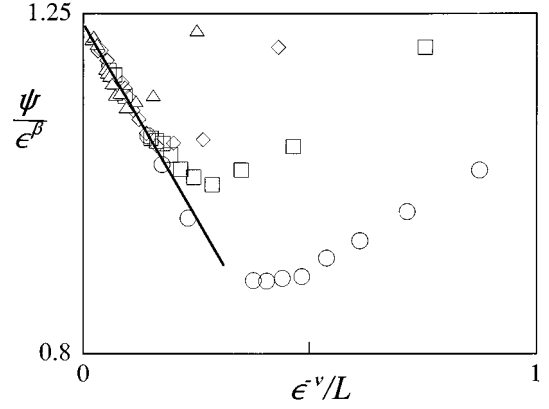


FIG. 12. A plot of  $\psi\varepsilon^{-0.27}$  versus  $\varepsilon^{-0.7}/L$  with  $T_\infty=1.3$ , as suggested by Eq. (15) for  $L_x=L_y=L$ . This plot contains all the available data for the squared layered system for different values of  $L$ , namely  $L=16$  ( $\circ$ ),  $40$  ( $\square$ ),  $70$  ( $\diamond$ ), and  $120$  ( $\times$ ). The line best fitting the data near the origin has slope  $-1.1$ , and extrapolates to  $B \approx 1.24$ , in accordance with the rest of the analysis.

The assumptions about the driving force, which is introduced as a relevant variable, seem to be at the origin of the failure of the presently accepted continuous version of the DLG. The latter involves a drift  $J(\phi) = a_0 + a_1\phi^2 + \dots$  which causes the nonequilibrium system to have the critical behavior of the Gaussian  $\phi^2$  model (with an indirect influence of  $\phi^4$ ). One should expect under such assumption for the drift that  $\langle J(\phi) \rangle \approx a(1 - m^2)$  with  $a$  independent of  $T$  sufficiently near (but excluding) the critical point [29]. However, the latter result does not seem to be supported by the plots in Fig. 14, where data (if the assumptions of the model are accepted) suggest a more complex behavior of  $J(\phi)$ .

#### IV. DISCUSSION

We have compared by MC simulations and kinetic mean-field theory the various phase transitions which are exhibited by the layered DLG,  $\Lambda_E$ , and by the standard DLG,  $\lambda_\infty$ , for half occupied lattices. The interest is in the (nonequilibrium)

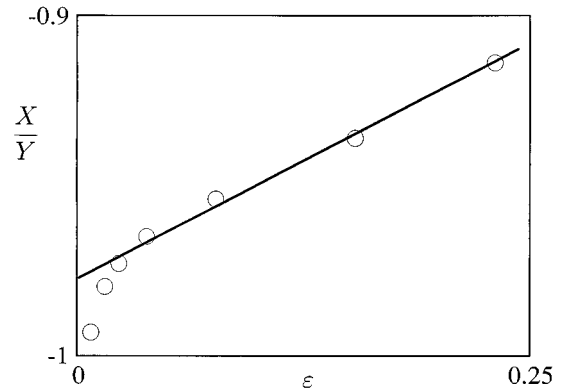


FIG. 13. Temperature dependence of dimensionless relation  $X(\varepsilon, u)/Y(\varepsilon, u)$  [cf. Eq. (12)] as obtained by the least squares method from data for  $m$  corresponding to different sizes (namely,  $2 \times 20 \times 20$ ,  $2 \times 26 \times 44$ ,  $2 \times 32 \times 82$ ,  $2 \times 40 \times 160$ ,  $2 \times 20 \times 16$ ,  $2 \times 26 \times 26$ ,  $2 \times 30 \times 36$ , and  $2 \times 40 \times 64$ ). The line is the empirical fit  $X/Y = 0.277\varepsilon - 0.977$  for  $\xi < L$ .



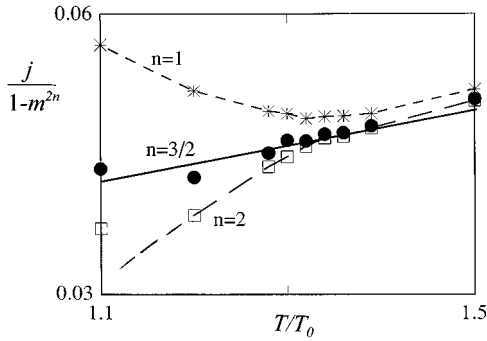


FIG. 14. Temperature dependence of the particle current divided by  $(1-m^{2n})$  from MC simulations, for different values of  $n$ , as indicated. Lines are a guide to the eye.

steady state which is obtained by a dynamical rule which reduces itself to the Metropolis algorithm for  $E=0$ .  $\Lambda_E$  exhibits two different phase transitions (Fig. 2). The one at  $T_\infty \equiv T_{E \rightarrow \infty} \approx 1.30$  is similar (for a saturating field) to the one at temperature  $T_\infty \approx 1.38$  in  $\lambda_\infty$ . That is, in addition to the fact that  $\Lambda_E$  exhibits (for  $\rho = \frac{1}{2}$ ) a configuration within each plane apparently indistinguishable from the one in  $\lambda_\infty$ , both systems are observed to be characterized by the same critical indexes, e.g.,  $\beta \approx 0.3$  (perhaps also  $\nu \approx 0.7$  with rather large error bars), and by the same scaling behavior over a wide range of values for  $T$  and  $L$ . The measured dependence of MC data on lattice shape and size is consistent with the existence of a unique correlation length which dominates at criticality, in spite of the fact that observed anisotropy of clusters might advise one considering two lengths in general.

The layered DLG exhibits another phase transition for any  $E$  at  $T_E^* < T_E$ . It has some similarities with the one in  $\Lambda_E$  for  $E=0$ , i.e., the equilibrium case. In particular, the liquid phase extends completely over one of the planes (for  $\rho = \frac{1}{2}$ ) so that no interface occurs independently of the value of  $E$ . Therefore, this is an interesting situation to be investigated. We have followed a hint from mean-field theory and found that a tricritical point occurs for  $E = E_c \approx 2$  ( $E_c = 3.5 \pm 0.1$  within the pair approximation) so that the phase transition is continuous for any  $E < E_c$ . The study of the critical point at  $T_E^*$  indicates that it belongs to the Ising universality class for any  $E$ . Summing up, a clear departure of  $\beta$  from the Onsager value is observed near  $T_\infty$ , when the system exhibits a linear liquid-vapor interface throughout the system along the direction of the applied field, while such departure is not observed within a similar critical region near  $T_E^*$ ,  $E < E_c$ , in the absence of the interface.

Our final conclusion is twofold. On the one hand, the present study suggests which basic ingredients are to be included in a field-theoretic version of the DLG and related systems, e.g., it seems that a drift which is relevant should not be invoked. The critical behavior of the DLG appears rather simple from the perspective of known results for other nonequilibrium lattice systems. That is, the observations above in the neighborhood of  $T_\infty$  and  $T_E^*$  may be interpreted as further evidence that the Ising critical point is rather robust [30]; only the presence of a peculiar linear interface (and not a driving field, which exists in the two situations investigated) is strong enough to induce a measurable anomaly near  $T_\infty$ . We believe this issue deserves further study. On the other hand, it is suggested that several systems (mentioned in Sec. I) belong to the universality class of the DLG. Therefore, experiments that focus on the nature of the (nonequilibrium) critical behavior of substances that could belong to this class would be of great interest. A specific question here is whether the observation  $\beta \approx 0.3$  is an actual characteristic of the class or an artifact, e.g., a difficult condition might give rise to an *effective exponent*. (It should be stressed that our MC analysis describes a well-defined scaling region with no indication of any crossover phenomena at all. However, variations of  $\beta$  from the above quoted value should not be ruled out if investigating even closer the critical point is finally allowed, e.g., in laboratory experiments.) Slow power-law decay of spatial correlations, as in (7), which is a feature of the DLG class [6], has been observed in a fluid whose walls are kept at different temperature [31]. More definite in characterizing the DLG class seems to be the presence of a linear interface or a similar anisotropic feature. The chances are that some low-dimensional conductors [7] and perhaps fluids under shear [32] are good examples. In relation with the latter, we mention that mean-field critical behavior [32] has been reported in accordance with field theory [33]. On the other hand, some *anomalies* reported for ionic fluids [34] might also be analyzed from this perspective, i.e., trying to identify there a nonequilibrium (steady) condition and a linear interface.

## ACKNOWLEDGMENTS

Financial support from DGICYT of Spain, Grant No. PB91-0709, and useful comments by Dr. K.T. Leung and Dr. R.K.P. Zia are acknowledged; we also thank Dr. J.S. Wang for communication of Ref. [18] before publication.

- [1] M.C. Cross and P.C. Hohenberg, *Rev. Mod. Phys.* **65**, 851 (1993).
- [2] D.H. Rothman and S. Zaleski, *Rev. Mod. Phys.* **66**, 1417 (1994).
- [3] J. Marro and R. Dickman, *Nonequilibrium Phase Transitions and Critical Phenomena in Lattice Systems* (Cambridge Univ. Press, Cambridge, in press).

- [4] S. Katz, J.L. Lebowitz, and H. Spohn, *J. Stat. Phys.* **34**, 497 (1984).
- [5] P.L. Garrido, J. Marro, and R. Dickman, *Ann. Phys. (N.Y.)* **199**, 366 (1990).
- [6] A. Achahbar and J. Marro, *J. Stat. Phys.* **78**, 1493 (1995)
- [7] See, for instance, J.B. Bates, J. Wand, and N.J. Dubney, *Phys. Today* **35**, 46 (1982), and references therein.

- [8] J.J. Alonso, P.L. Garrido, J. Marro, and A. Achahbar, *J. Phys. A* **28**, 4669 (1995).
- [9] A. Achahbar, P.L. Garrido, and J. Marro, *Molec. Phys.* (to be published).
- [10] K. Gawadzki and A. Kupiainen, *Nucl. Phys. B* **269**, 45 (1986).
- [11] H.K. Janssen and B. Schmittmann, *Z. Phys. B* **64**, 503 (1986).
- [12] K.T. Leung and J.L. Cardy, *J. Stat. Phys.* **44**, 567 (1986).
- [13] K. Binder and J.S. Wang, *J. Stat. Phys.* **55**, 87 (1989).
- [14] K.T. Leung, *Phys. Rev. Lett.* **66**, 453 (1991); see also K.T. Leung, *Int. J. Mod. Phys. C* **3**, 367 (1992).
- [15] B. Schmittmann and R.K.P. Zia, in *Phase Transitions and Critical Phenomena*, edited by C. Domb and J.L. Lebowitz (Academic Press, New York, 1995).
- [16] J.L. Vallés and J. Marro, *J. Stat. Phys.* **49**, 89 (1987).
- [17] J.S. Wang, K. Binder, and J.L. Lebowitz, *J. Stat. Phys.* **56**, 783 (1989).
- [18] J.S. Wang, *J. Stat. Phys.* **82**, 1409 (1996).
- [19] F.J. Alexander, I. Edrei, P.L. Garrido, and J.L. Lebowitz, *J. Stat. Phys.* **68**, 497 (1992).
- [20] J.L. Vallés, *J. Phys. (France) I* **2**, 1361 (1992).
- [21] C.K. Chan and L. Lin, *Europhys. Lett.* **11**, 13 (1990).
- [22] Z. Cheng, P.L. Garrido, J.L. Lebowitz, and J.L. Vallés, *Europhys. Lett.* **14**, 507 (1991).
- [23] E. Praestgaard, H. Larsen, and R.K.P. Zia, *Europhys. Lett.* **25**, 447 (1994).
- [24] C. Yeung, T. Rogers, A. Hernández-Machado, and D. Jasnow, *J. Stat. Phys.* **66**, 1141 (1992).
- [25] J. Kertész and T. Vicsek, in *Fractals in Science*, edited by A. Bunde and S. Havlin (Springer-Verlag, Berlin, 1994), p. 89.
- [26] K.T. Leung and R.K.P. Zia, *J. Phys. A* **26**, L737 (1993).
- [27] *Finite-Size Scaling*, edited by J.L. Cardy (North-Holland, Amsterdam, 1988).
- [28] *Finite Size Scaling and Numerical Simulation of Statistical Systems*, edited by V. Privman (World Scientific, Singapore, 1990).
- [29] N.G. van Kampen, *Stochastic Processes in Physics and Chemistry* (North-Holland, Amsterdam, 1981).
- [30] G. Grinstein, C. Jayaprakash, and Y. He, *Phys. Rev. Lett.* **55**, 2527 (1985).
- [31] B.M. Law, P.N. Segré, R.W. Gammon, and J.V. Sengers, *Phys. Rev. A* **41**, 826 (1990).
- [32] D. Beysens and M. Gbadamassi, *Phys. Rev. A* **22**, 2250 (1980).
- [33] A. Onuki, K. Yamazaki, and K. Kawasaki, *Ann. Phys. (N.Y.)* **131**, 217 (1981).
- [34] J.M.H. Levelt Sengers and J.A. Given, *Mol. Phys.* **80**, 899 (1993).